Contents lists available at YXpublications

International Journal of Applied Mathematics in Control Engineering

Journal homepage: http://www.ijamce.com

Bionic Variable Structure UAV Design and Flight Control

Yue Zan[a], Xingguo Song[b,*], Lulu Gong[a], Qiu Hou[a], Jie Tang[a]

[a] Southwest Jiaotong University, Department of Mechanical Engineering.

[b] Southwest Jiaotong University, Artificial Intelligence and Robotics Research

ARTICLE INFO

Article history:
Received 12 January 2023
Accepted 21 February 2023
Available online 28 February 2023

Keywords:
UAV
Variable structure
Mathematical modeling
Flight Control

ABSTRACT

Aiming at the diverse application scenarios of quadrotor UAVs in disaster environments, a novel type of quadrotor UAV with variable structure folding is proposed based on mathematical model analysis of quadrotor UAVs. The objective is to address the size problem of UAVs in different application environments and enhance their adaptability and obstacle avoidance capability. The structural scheme of the variable structure quadrotor UAV is studied in detail, and the kinematics and dynamics model of the variable structure quadrotor UAV under deformation is constructed. Furthermore, the control method of the variable structure UAV platform is investigated based on the double-loop PID control principle. Through the construction of a prototype and flight experiments, the feasibility and advantages of the proposed UAV in various confined spaces are verified. The results indicate that the UAV has a maximum stable rotational flight angle of 60° and foldable capability. The design scheme and concept proposed in this study have research significance for future folding schemes of variable structure UAVs.

1. Introduction

Quadcopter UAVs are extensively employed in military and civilian applications for environmental exploration and detection tasks in various extreme environments due to their simple structure, versatility, and strong environmental adaptability(Mintchev & Floreano, 2016). The majority of quadrotor UAVs currently in use have fixed frames, which require different sizes for different application scenarios, significantly reducing the cost-effectiveness of the quadrotor (Tuna et al., 2020). We draw inspiration from nature, where flying avian species fold their wings to alter their width when passing through a narrow gap, allowing them to glide through the gap seamlessly. Through the investigation of birds' wing folding process, we discovered that birds achieve higher flight rates, smaller flight areas, and longer flight envelopes(Chen & Yeh, 2021; Di Luca et al., 2017; Floreano et al., 2017) by tapping down the folded wings. The unique behavior of birds folding their wings to pass through slits of varying sizes has piqued the interest of researchers and has led to the emergence of the concept of folding quadrotor drones(Badr et al., 2019; Fabris et al., 2022; Jitsukawa et al., 2017; Ryu et al., 2020). With the development of intelligent deformation technology for UAVs, which encompasses multiple fields such as structure theory, control, aerodynamics, and materials, the intelligent variable structure UAV has become the most innovative subject in the military and civilian fields of UAVs in recent years.

To address the issue of the center of gravity position and inertia tensor of UAVs changing with varying loads, Chanyoung Kim designed a variable structure UAV that monitors the real-time changes in the center of gravity position and inertia tensor of the UAV through adaptive control methods (Kim et al., 2021).The orientation of the quadrotor is then adjusted to ensure stable flight control of the UAV. However, this method may not be adaptable to different flight environments when carrying weight and maintaining stable flight states.

The High Performance Robotics Lab at UC Berkeley has developed a passive hinge structure that allows drones to navigate through gaps(Bucki & Mueller, 2019). This passive deformation design relies heavily on the UAV's trajectory generation algorithm, but there is still a significant risk of collision when the positioning is inaccurate.

Na Zhao et al. proposed a quadrotor UAV with a scalable structure based on a scissor shape(Zhao et al., 2017). This design has minimal aerodynamic impact and exhibits excellent flight adaptability and obstacle-crossing capability. However, in reality, the hardware

* Corresponding author.
E-mail addresses: songxg@swjtu.edu.cn (X. Song)
doi:

equipment such as flight control and sensors located at the center of the quadcopter UAV frame has a certain physical volume, which imposes limits on the scalability of this structure.

Davide Falanga has designed and developed a UAV platform that does not require a symmetrical form and is self-adapting to any state during flight, whether passing through a slit or in a loaded transport state, by developing control strategies (Falanga et al., 2019). This platform features four rotors rotating around the Z-axis, with the minimum retractable state being the H-form. However, in the H-form state, the propellers on both sides produce a certain degree of interference and airflow disturbance, limiting the minimum width of the UAV platform to the sum of the diameters of the two propeller blades.

In this paper, we design a new cross-shaped quadrotor UAV(Negrello et al., 2016) that rotates around the X-axis. The left and right arms of the UAV are connected to the main body through a servo, allowing for remote control of the arm rotation and the contraction of the drone for crossing narrow slits. To ensure stable flight during hovering, we mathematically model the airframe(Haoqin et al., 2015; Hu et al., 2021; Mahony et al., 2012; Vargas et al., 2015), and combine it with a dual-loop PID control strategy(Mou et al., 2016; Sen & Zhongsheng, 2017), optimize the UAV attitude and calculate the required RPM for stabilization.

2. Bionic Variable Structure UAV System Description

2.1 Mechanical design

In flying birds, the humerus and ulna are connected by tendons to extend and fold the wings during flight. After observing the characteristics of contracted wings of birds and considering the safety and aerodynamic characteristics of the UAV in flight, we propose a bionic variable structure quadrotor UAV with folding rotor around the X-axis of the UAV. The design prototype presented in this project is a traditional cross-type quadrotor UAV frame. The whole frame is made of carbon fiber plate, which has the feature of light weight and high strength, and increases the strength of the quadrotor UAV while significantly reducing the overall mass of the airframe. The schematic diagram of the prototype aircraft is shown in Figure 1. The whole aircraft fuselage is designed with 250mm wheelbase, and the overall dimensions of the aircraft are 400mm×473mm×46mm, and the weight of the whole aircraft is 1.5kg.

Fig. 1. Variable structure UAV quadrotor model

Fig. 2. Rotor shoulder mechanism

On the left and right sides of the UAV we designed a kind of axle shoulder, which was made by 3D printing, as shown in Figure 2. During the flight, the axle shoulder is fixed to the servo LX-224HV to control the rotation of the left and right wing parts to realize the control of the flight attitude of the variable structure UAV. For the non-folding rotor part, we use a one-piece design, which increases the overall strength of the system and makes the quadcopter drone more stable compared to the traditional quadcopter drone frame.

The proposed variable structure UAV in this paper can actively change its flight attitude during flight, which in turn achieves changing the size and shape of the overall UAV so as to pass through narrow gaps or extreme disaster environments with different flight attitudes, as shown in Figure 3. The process of structural drones flying over different environments such as tunnels and slits is divided into three main phases: preparation phase, structural deformation phase and structural recovery phase.

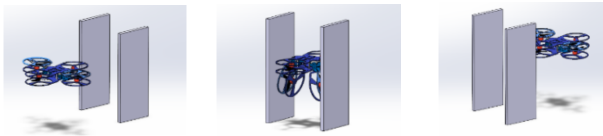

Fig. 3. Schematic diagram of the drone crossing the slit obstacle, where the leftmost diagram shows the preparation phase of the variable structure drone, the middle diagram shows the structure deformation phase, and the rightmost diagram shows the structure recovery phase.

After detecting special environments that are unsafe or obstructed to pass through, such as tunnel pipes and slit passages, the drone flies steadily, hovers at a fixed point, and then flies across after reducing the width of the drone by controlling the rotation of the rudder to make it meet the size requirements for crossing special environments. After safely passing through the channel or slit the drone returns to the cross-shaped drone form and completes the entire crossing flight process.

Define the angle between the wing and the Z-axis of the body coordinate system of the UAV as δ, which is the rotation angle of the rudder relative to the frame. During the deformation process, the left and right wings rotate around the X-axis with the rudder as the origin, and the lateral dimension of the vehicle decreases as the tilt angle of the rudder becomes larger, which in turn improves the slit passage rate of the vehicle.

The relationship between the lateral dimension of the arm and the rotation angle of the rudder is:

$$b = 2l_a \cos\delta + l_b \tag{1}$$

l_a indicates the length of the left and right arms, l_b indicates the width of the body, $\delta \in [0^\circ, 90^\circ)$.Theoretically, the rotation angle can be infinitely close to 90 degrees, but the larger the rotation angle in flight, the greater the power loss of the vehicle, and the flight state is unstable, so the actual servo rotation angle should be less than 90°.

2.2 Hardware Structure

This section introduces the electronic components and mechanical parts of the system. Since the folding mechanism causes power loss, in order to obtain higher thrust while reducing the size of the UAV, the T-MotorV2007-2550KV motor and T5046 propeller were used for this project to match. Up to 12.27N of thrust per motor. Although the PWM servo can instantly complete the angle change, but its accuracy is poor and the use of time will grow with the use of the phenomenon of false gear. Therefore, we use Mirage LX-224HV bus servo for our axis shoulder servo, which is suitable for various bionic robot joints. Its operating voltage is 6~8.4v, servo precision 0.3°, UART serial command control, communication baud rate 115200, with two modes of servo and gear motor. Each servo can provide a torque of 20kg/cm, which can withstand the torque provided by the rotor to the servo during the flight to complete the folding purpose.

In order to effectively and precisely control the servo on the shoulder part of the axis, the Arduino Mega 2560 was selected to communicate with the servo through the serial port and mapped to the six channels of the UAV remote control for retracting and unfolding the flight in different scenes.

The overall mass of the designed quadrotor UAV is 1.5KG, the UAV axis distance is 250mm, the selected format TATTU capacity 2300MAH, voltage 14.8V, discharge rate 45C, and weight 236g. At this time the system flight time is about 12 minutes. The complete mechanical part component parts are shown in Table 1.

Tab. 1. Variable structure quadrotor UAV hardware selection

Component parts	Model	Parameters
Motor	T-MotorV2007	2550KV
Propeller	T5046	
Servo	Hiwonder	LX-224HV
Servo driver board	Hiwonder	
Servo control board	Arduino	Mega 2560
Drone flight control	Pixhawk	2.4.8
ESC	HSKRC	45A

3. Mathematical Model

Due to the special and variable nature of the deformed UAV, it is necessary to conduct comprehensive control and simulation tests based on the mathematical model of the variable-structure quadrotor UAV. The variable-structure quadrotor UAV is simplified to the following form.

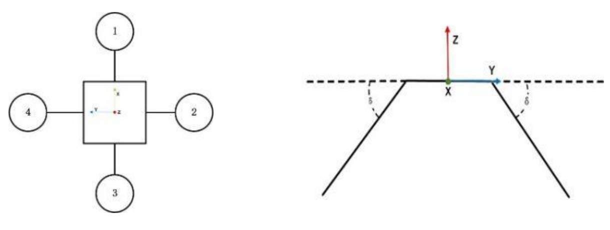

Fig. 4. The figure shows the analysis schematic of the variable structure UAV model, with the top view on the left and the main view on the right

It can be seen that the design consists of two main parts: 1) the two front and rear rotor blades and the central body that carries the control system, and 2) two wings rotating around the X-axis of the body, controlled by bus servos. When the quadrotor UAV flight encounters a narrow gap, the left and right rotors rotate downward δ to change the UAV form and axis distance, so that the quadrotor UAV flight through the narrow gap. A total of six coordinate systems are used in the model building process. where the earth coordinate system fixed to the ground is defined as $\mathrm{O_e}X_eY_eZ_e$ as shown in the figure. Fixed at the center of the UAV body is the body coordinate system $O_bX_bY_bZ_b$. Finally, four rotor coordinate systems fixed at the center of the rotor are defined as $O_{R,i}X_{R,i}Y_{R,i}Z_{R,i}$ where i represents the i-th rotor, $i \in \{1,2,3,4\}$.

To simplify the model, the following assumptions are made:

1) The drone body is a uniformly symmetric rigid body
2) The geometric center of the drone coincides with the center of gravity.
3) Rotor thrust and torque proportional to the square of the rotor speed.
4) The thrust and drag torque generated by the propeller are independent of the thrust and drag torque of the other rotors, and the resulting airflow does not interfere with each other.
5) The drone is only subject to gravity and propeller pull in the vertical direction.

For the above assumptions to some extent ignore the realistic flight characteristics that may have an impact on the vehicle, so we consider the impact of airflow between the rotors of the UAV as a disturbance to the airframe and subsequently use the control system to eliminate its impact on the UAV.

3.1 Kinematic Modeling

The rotation matrix R_b^e represents the rotation of any vector from the earth coordinate system $\mathrm{O_e}X_eY_eZ_e$ to the UAV body coordinate system $O_bX_bY_bZ_b$.

$$R_b^e = \begin{bmatrix} cos\theta cos\psi & cos\psi sin\theta sin\phi - sin\psi cos\phi & cos\psi sin\theta cos\phi + sin\psi sin\phi \\ cos\theta sin\psi & sin\psi sin\theta sin\phi + cos\psi cos\phi & sin\psi sin\theta cos\phi - cos\psi sin\phi \\ -sin\theta & sin\phi cos\theta & cos\phi cos\theta \end{bmatrix} \quad (2)$$

We assume that the thrust f generated by each rotor is proportional to the torque τ to the square of the rotational speed ω, so the following equation relationship exists.

$$\begin{cases} \mathrm{f} = \mathrm{C_t} \cdot \omega^2 \\ \tau = \mathrm{C_m} \cdot \omega^2 \end{cases} \quad (3)$$

$\mathrm{C_t}$ represents the lift coefficient and $\mathrm{C_m}$ represents the drag moment coefficient.

The rigid body kinematic model of the variable structure UAV is as follows：

$$\begin{cases} \dot{P^e} = V^e \\ \dot{\Theta} = W \cdot \Omega^b \\ P^e = [x \quad y \quad z]^T \\ V^e = [u \quad v \quad w]^T \\ \Omega^b = [p \quad q \quad r]^T \end{cases} \quad (4)$$

P^e represents the three-axis position of the UAV in the earth coordinate system, V^e represents the three-axis linear velocity of the UAV in the earth coordinate system, and Ω^b represents the three-axis angular velocity of the UAV in the earth coordinate system.

$$\mathrm{W} = \begin{bmatrix} 1 & tan\theta sin\phi & tan\theta cos\phi \\ 0 & cos\phi & -sin\phi \\ 0 & \dfrac{sin\phi}{cos\theta} & \dfrac{cos\phi}{cos\theta} \end{bmatrix} \quad (5)$$

In the case of small perturbation, the rate of change of attitude angle is approximately equal to the rotational angular velocity, so it is simplified as：

$$\begin{bmatrix} \dot{\phi} \\ \dot{\theta} \\ \dot{\psi} \end{bmatrix} = \begin{bmatrix} p \\ q \\ r \end{bmatrix} \quad (6)$$

3.2 Dynamical model

Because of the versatility of variable structure UAVs, their models are more complex compared to traditional quadrotor UAVs. From the Newton-Euler method we know that the motion of a rigid body is the translational motion and rotation around the center of mass. Therefore, the dynamics of the body is modeled in the following form.

$$\begin{bmatrix} F^e \\ M^b \end{bmatrix} = \begin{bmatrix} 0 \\ \Omega^b \times J_B \cdot \Omega^b \end{bmatrix} + \begin{bmatrix} m \cdot \dot{V^e} \\ J_B \cdot \dot{\Omega^b} \end{bmatrix} \quad (7)$$

J_B represents the total inertia matrix of the UAV. The components of the body are usually simplified into simple assemblies to facilitate the calculation of the rotational inertia and inertia products to obtain the rotational inertia tensor. Suppose the fuselage is a rectangular body with length and width l_b and height h_b, the arm is a rectangular body with length l_a, width w_a and height h_a, the rotor is a cylinder with radius r_r and height h_r, and the motor is a cylinder with radius r_m and height h_m, so the inertia of rotation of each part is calculated as shown below.

$$\begin{cases} J_b = \frac{m_b}{12} diag\{h_b^2 + l_b^2, h_b^2 + l_b^2, l_b^2 + l_b^2\} \\ J_{a,i} = \frac{m_a}{12} diag\{w_a^2 + h_a^2, l_a^2 + h_a^2, w_a^2 + l_a^2\} \\ J_r = \frac{m_r}{12} diag\{3r_r^2 + h_r^2, 3r_r^2 + h_r^2, 6r_r^2\} \\ J_m = \frac{m_m}{12} diag\{3r_m^2 + h_m^2, 3r_m^2 + h_m^2, 6r_m^2\} \end{cases} \tag{8}$$

Due to the special nature of variable structure UAV folding, the motor, rotor and arm rotate relative to the X-axis in the body coordinate system $O_bX_bY_bZ_b$. so their rotational inertia also needs to change in real time with the rotation of the servo. Introduce the rotation matrix for its representation:

$$\begin{cases} J'_{a,i} = R_x(\delta) J_{a,i} R_x^T(\delta) \\ J'_r = R_x(\delta) J_r R_x^T(\delta) \\ J'_m = R_x(\delta) J_m R_x^T(\delta) \end{cases} \tag{9}$$

The rotation matrix is shown below:

$$R_x(\delta) = \begin{bmatrix} 1 & 0 & 0 \\ 0 & cos\delta & -sin\delta \\ 0 & sin\delta & cos\delta \end{bmatrix} \tag{10}$$

At this point the overall inertia tensor varies with the body, so the overall inertia tensor can be expressed as

$$J_B = \mathrm{J_b} + \sum_{i=1}^{4} J_{a,i} + J_r + J_m \tag{11}$$

Assuming that the vehicle is subjected to only gravity and propeller pull, from equation 7 we can model the position dynamics of the UAS as follows.

$$\begin{cases} m\dot{V}^e = G^e - f^e \\ f^e = R_b^e \cdot f^b \end{cases} \tag{12}$$

f^e is expressed as the lift generated by the rotor relative to the earth coordinate system, and f^b is expressed as the lift generated by the rotor relative to the airframe coordinate system. The positional dynamics modeling results can be obtained by simplifying the above equation.

$$\begin{cases} \dot{u} = -\frac{f^b}{m}(cos\psi sin\theta cos\phi + sin\psi sin\phi) \\ \dot{v} = -\frac{f^b}{m}(sin\psi sin\theta cos\phi - cos\psi sin\phi) \\ \dot{w} = g - \frac{f^b}{m} cos\phi cos\theta \end{cases} \tag{13}$$

From equation 7 we can model the attitude dynamics of the UAS:

$$\begin{cases} M^b = \Omega^b \times J_B \cdot \Omega^b + J_B \cdot \dot{\Omega}^b \\ M^b = G^a + \tau \\ G^a = \begin{bmatrix} J_{RP} q(\omega_1 - \omega_2 + \omega_3 - \omega_4) \\ J_{RP} P(-\omega_1 + \omega_2 - \omega_3 + \omega_4) \\ 0 \end{bmatrix} \end{cases} \tag{14}$$

$\tau = [\tau_x \quad \tau_y \quad \tau_z]^T$ represents the lift distance generated by the rotor, G^a represents the gyroscopic moment generated by the quadrotor UAV, and J_{RP} is the total rotational inertia of the motor rotor and propeller around the rotational axis of the body. And for the dynamics model it is known that $\dot{\Omega}^b = [\dot{p} \quad \dot{q} \quad \dot{r}]^T$ and the attitude dynamics modeling results can be obtained by simplifying the above equation

$$\begin{cases} \dot{p} = \frac{1}{J_{xx}}[\tau_x + qr(J_{yy} - J_{zz}) - J_{RP} q\Omega] \\ \dot{q} = \frac{1}{J_{yy}}[\tau_y + pr(J_{zz} - J_{xx}) + J_{RP} p\Omega] \\ \dot{r} = \frac{1}{J_{zz}}[\tau_z + pq(J_{xx} - J_{yy})] \end{cases} \tag{15}$$

Where $\Omega = -\omega_1 + \omega_2 - \omega_3 + \omega_4$.

Combine the position dynamics model and attitude dynamics model with the kinematic model, and let $\begin{bmatrix} U_1 \\ U_2 \\ U_3 \\ U_4 \end{bmatrix} = \begin{bmatrix} f^b \\ \tau_x \\ \tau_y \\ \tau_z \end{bmatrix}$.

we can get the nonlinear six degrees of freedom model of the variable structure quadrotor UAV. The equations x、y、z represent the position of the UAV, and the equations ϕ、θ、ψ reflect the attitude of the UAV. Observing the model we can find that the attitude equations are coupled to each other and the position equations are related to the attitude, so the whole system is in a strongly coupled state.

$$\begin{cases} \ddot{x} = -\frac{U_1}{m}(cos\psi sin\theta cos\phi + sin\psi sin\phi) \\ \ddot{y} = -\frac{U_1}{m}(sin\psi sin\theta cos\phi - cos\psi sin\phi) \\ \ddot{z} = g - \frac{U_1}{m} cos\phi cos\theta \\ \ddot{\phi} = \frac{1}{J_{xx}}[U_2 + qr(J_{yy} - J_{zz}) - J_{RP} q\Omega] \\ \ddot{\theta} = \frac{1}{J_{yy}}[U_3 + pr(J_{zz} - J_{xx}) + J_{RP} p\Omega] \\ \ddot{\psi} = \frac{1}{J_{zz}}[U_4 + pq(J_{xx} - J_{yy})] \end{cases} \tag{16}$$

4. Flight Control

For the control system of the UAV the classical two-loop PID control is used here, thus realizing the positional control of the variable structure quadrotor. Compared with other methods, the series dual-loop PID has remarkable features such as simple control structure, stable system and easy implementation. Based on the mathematical model established in this paper for the variable structure UAV, the system is brought to a more stable state by adjusting the control parameters so that it can perform stable hovering and flight control. The attitude controller is used as the inner loop control of the system, and the position controller is used as the outer loop control of the system. The block diagram of the control system is shown in Figure 5.

For the quadrotor speed loop with variable structure, the design is as follows:

$$\begin{cases} U_x = K_{p,x} e_x + K_{i,x} \int e_x dt + K_{d,x} \dot{e_x} \\ U_y = K_{p,y} e_y + K_{i,y} \int e_y dt + K_{d,y} \dot{e_y} \\ U_z = K_{p,z} e_z + K_{i,z} \int e_z dt + K_{d,z} \dot{e_z} \end{cases} \tag{17}$$

$K_{p,x}$ $K_{p,y}$ $K_{p,z}$ are the proportional control coefficients in the PID controller, $K_{i,x}\,K_{i,y}\,K_{i,z}$ is the control coefficient of the integral term in the PID controller, $K_{d,x}\,K_{d,y}\,K_{d,z}$ are the differential term control coefficients in the PID controller. $U_x U_y U_z$ is the virtual control volume. $e_x e_y e_z$ is divided into the position error of the UAV in x、y、z directions.

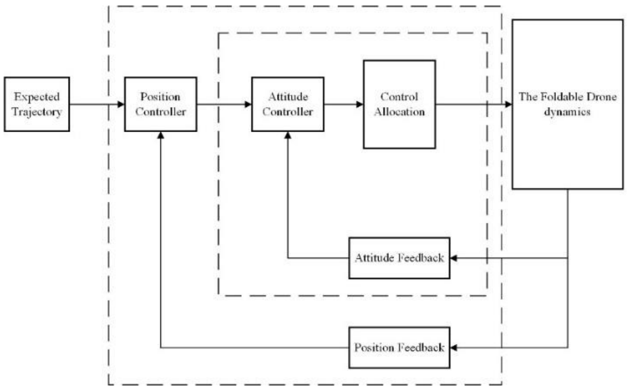

Fig. 5. The figure shows the Control block diagram of variable structure UAV system

And for attitude control not only to control the stable attitude of the UAV, but also to consider the further control of the attitude stability of the UAV based on the rotor rotation. The pitch and roll of the UAV is first controlled based on a conventional control vehicle with an attitude control loop, designed as follows.

$$\begin{cases} U_\phi = K_{p,\phi}\, e_\phi + K_{i,\phi} \int e_\phi dt + K_{d,\phi}\, \dot{e_\phi} \\ U_\theta = K_{p,\theta}\, e_\theta + K_{i,\theta} \int e_\theta dt + K_{d,\theta}\, \dot{e_\theta} \\ U_\psi = K_{p,\psi}\, e_z + K_{i,\psi} \int e_\psi dt + K_{d,\psi}\, \dot{e_\psi} \end{cases} \tag{18}$$

e_ϕ、e_θ、e_z are the attitude errors of the UAV in the cross-roll, pitch, and yaw directions, respectively.

The variable structure UAV designed in this paper will go through three stages of flight before deformation, flight during deformation and flight after deformation in the whole flight process.

The flight attitude and position of the drone are mainly controlled by the four rotors of the drone and the servos on both sides of the left and right rotors. In the UAV deformation flight, using control distribution to adjust the flight attitude of the UAV, based on the previous force analysis, we can get the relationship between the control distribution expectation and the expected moment:

$$\begin{cases} U_1 = C_t({\omega_1}^2 + {\omega_2}^2 + {\omega_3}^2 + {\omega_4}^2) \\ U_2 = C_t l_a \cos^2\delta\,({\omega_4}^2 - {\omega_2}^2) \\ U_3 = C_t l_a({\omega_3}^2 - {\omega_1}^2) \\ U_4 = C\_m({\omega_1}^2 - {\omega_2}^2 + {\omega_3}^2 - {\omega_4}^2) \end{cases} \tag{19}$$

The control distribution equation is obtained:

$$\mathrm{U} = \begin{bmatrix} 1 & 1 & 1 & 1 \\ 0 & -\cos^2\delta & 0 & \cos^2\delta \\ -1 & 0 & 1 & 0 \\ 1 & -1 & 1 & -1 \end{bmatrix} \begin{bmatrix} {\omega_1}^2 \\ {\omega_2}^2 \\ {\omega_3}^2 \\ {\omega_4}^2 \end{bmatrix} \tag{20}$$

It can be seen that the control assignment matrix C changes gradually with the angle of deformation, and the full rank of the matrix C appears only when $\delta = 90°$. And for the present model, the whole deformation process does not involve the position of the singularity point $\delta = 90°$.

5. Experiment

5.1 Deformation hovering flight experiment of variable structure UAV

In order to verify the feasibility of the proposed variable structure UAV, we built and fabricated a prototype of the variable structure UAV based on the designed mechanical structure and model analysis, as shown in Figure 6. The total mass of the variable structure UAV is 1.5kg and the radius of the fuselage is 240mm. Experiments were conducted to test the throttle lift test and the flight deformation function in different environments for the UAV.

Fig. 6. Variable structure UAV prototype model

In order to verify the feasibility of the variable structure quadrotor UAV, the deformation function and hovering flight test are performed for the fabricated prototype. In the deformation hovering flight experiment, the left and right rotors are required to achieve stable hovering of the UAV at a certain height when rotating at different angles. The rotor rotation angle is slowly increased to 10° rotation angle as a group, and each group of experiments is tested three times, thus eliminating the chance of flight experiment stability.

Figure 7 shows the hovering flight test process of the variable structure UAV, with the rotor angle gradually tilted from 0° to 60°. From the flight illustration, it can be seen that the UAV flew stably during the rotational deformation process. At a tilt angle of 0° to 50°, the flight altitude of the UAV is essentially constant. When rotating to 60°, the flight altitude of the drone decreases, and it is necessary to increase the throttle for adjustment. There are two main reasons for this phenomenon: firstly, because as the rotation angle increases, the force generated by the UAV rotor needs to be decomposed and then transformed into upward lift, and the rest of the decomposed force we call lift loss. So the larger the rotation angle, the greater the lift loss. The second is the altitude loss due to the aerodynamic interference between the rotors of the vehicle. When the rotation angle is small, the aerodynamic interference is small and can be considered negligible, but when the angle is large, the aerodynamic interference also causes a certain amount of lift loss. Due to the above two reasons, when the rotation angle of the rotor of the vehicle exceeds 60°, it will cause a large loss of lift and a certain degree of decrease in flight height.

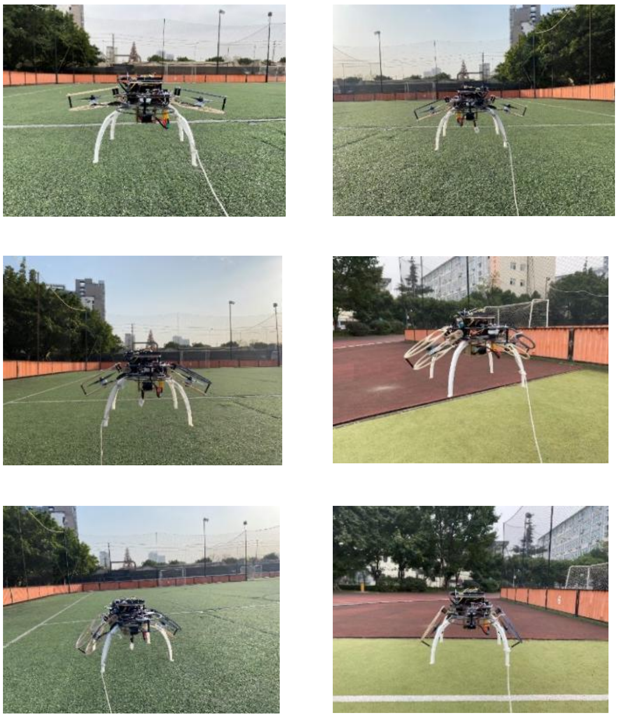

Fig. 7. This image shows the stable hovering state of a variable structure UAV rotor under different rotation angles. Folding and deforming stable flight experiment of UAV in a group of 10°. The above figure indicates the hovering state of the UAV under the rotation angle of 10°~60° respectively.

5.2 Slit and simulated tunnel leap experiments

In order to verify the flight capability of the designed variable structure UAV under special environment, flight experiments of simulated slit and simulated tunnel were conducted for the variable structure UAV.

Figure 8 shows the action sequence of the variable structure UAV traversing the simulated slit channel experiment. The width of the simulated slit is 500 mm, and the rotor rotation angle of the UAV is 50°.Before the flight experiment, after hovering the UAV smoothly, the UAV is propelled forward to form a certain angle with the ground to provide power in the X direction, which makes the UAV fly forward. From the illustration of the flight process, it can be seen that the UAV has the ability to traverse the slit.

Fig. 8. The figure shows a simulated slit flight experiment of a variable structure UAV with a slit distance of 500 mm. the leftmost figure shows the preparation stage before starting the UAV crossing the slit. After the structure is deformed, the UAV crosses the slit and finally passes through the slit safely to achieve the purpose of improving the crossing ability.

In order to verify that it can traverse the pipeline and has the ability to carry out special work in the pipeline, a simulated pipeline platform is designed and built, the size of the simulated pipeline is 500mm×500mm×500mm, and the platform device is shown in the figure below.

Fig. 9. The figure shows the flight experiment simulation pipeline platform, the pipe size is 500mm×500mm×500mm.

In the leap simulation pipe experiment, the rotor of the vehicle rotates at an angle of 50°, and after the vehicle stabilizes and hovers, the rotor is controlled to propel the UAV forward. In the experiment, the variable structure UAV flew stably and could cross the pipeline stably. Figure 10 shows the action sequence of the variable structure UAV leaping over the pipeline. The experimental results show that the UAV has the ability to traverse the pipeline and can perform special work in the pipeline.

Fig. 10. The picture shows a simulated pipeline flight experiment of a variable structure UAV. The left side shows the prepared attitude of the UAV before crossing the pipeline, flying smoothly into the pipeline after deformation and folding, and finally flying out.

The flight experiment results show that the UAV can fly stably at a rotation angle of 0° to 60°, and the flight height of the UAV will drop when the rotation angle of the rotor is too large. The experimental results verify that the variable structure UAV designed in this paper has the ability to traverse slits and perform special work inside the pipeline.

6. Summary

This paper proposes a novel variable structure quadrotor UAV that can adapt to special environments and overcome limitations in size. The UAV achieves this by reducing its lateral size through the rotation of its left and right rotors, enabling it to traverse slits and other challenging environments. To validate the feasibility of the proposed design, we analyze and model the dynamics of the variable structure UAV and conduct experimental tests to demonstrate that the rotor rotation angles do not compromise lift capacity. The prototype of the variable structure UAV is designed and built, and flight tests confirm its stability at rotor rotation angles of up to 60°. These results highlight the potential of the variable structure quadrotor UAV for applications in disaster rescue, tunnel exploration, and beyond.

References

Badr, S., Mehrez, O., & Kabeel, A. E. (2019). A design modification for a quadrotor UAV: Modeling, control and implementation. Advanced Robotics, 33(1), 13–32.

Bucki, N., & Mueller, M. W. (2019). Design and Control of a Passively Morphing Quadcopter. 2019 International Conference on Robotics and Automation (ICRA), 9116–9122.

Chen, W.-H., & Yeh, S.-I. (2021). Aerodynamic effects on an emulated hovering passerine with different wing-folding amplitudes. Bioinspiration & Biomimetics, 16(4), 046011.

Di Luca, M., Mintchev, S., Heitz, G., Noca, F., & Floreano, D. (2017). Bioinspired morphing wings for extended flight envelope and roll control of small drones. Interface Focus, 7(1), 20160092.

Fabris, A., Aucone, E., & Mintchev, S. (2022). Crash 2 Squash: An Autonomous Drone for the Traversal of Narrow Passageways. Advanced Intelligent Systems, 4(11).

Falanga, D., Kleber, K., Mintchev, S., Floreano, D., & Scaramuzza, D. (2019). The Foldable Drone: A Morphing Quadrotor That Can Squeeze and Fly. IEEE Robotics and Automation Letters, 4(2), 209–216.

Floreano, D., Mintchev, S., & Shintake, J. (2017). Foldable drones: From biology to technology (M. Knez, A. Lakhtakia, & R. J. Martín-Palma, Eds.; p. 1016203).

Haoqin, S., Zhan, H., Xiaoxiang, B., Hongwei, S., & Jing, S. (2015). Morphing Process Research of UAV with PID Controller. Procedia Engineering, 99, 873–877.

Hu, D., Pei, Z., Shi, J., & Tang, Z. (2021). Design, Modeling and Control of a Novel Morphing Quadrotor. IEEE Robotics and Automation Letters, 6(4), 8013–8020.

Jitsukawa, T., Adachi, H., Abe, T., Yamakawa, H., & Umezu, S. (2017). Bio-inspired wing-folding mechanism of micro air vehicle (MAV). Artificial Life and Robotics, 22(2), 203–208.

Kim, C., Lee, H., Jeong, M., & Myung, H. (2021). A Morphing Quadrotor that Can Optimize Morphology for Transportation (arXiv:2108.06759). arXiv.

Mahony, R., Kumar, V., & Corke, P. (2012). Multirotor Aerial Vehicles: Modeling, Estimation, and Control of Quadrotor. IEEE Robotics & Automation Magazine, 19(3), 20–32.

Mintchev, S., & Floreano, D. (2016). A pocket sized foldable quadcopter for situational awareness and reconnaissance. 2016 IEEE International Symposium on Safety, Security, and Rescue Robotics (SSRR), 396–401.

Mou, Y., Zhang, Q., Liu, S., & Liang, K. (2016). The Flight Control of Micro Quad-Rotor UAV Based on PID. 2016 31st Youth Academic Annual Conference of Chinese Association of Automation (Yac), 353–356.

Negrello, F., Silvestri, P., Lucifredi, A., Guerrero, J. E., & Bottaro, A. (2016). Preliminary design of a small-sized flapping UAV: II. Kinematic and structural aspects. Meccanica, 51(6), 1369–1385.

Ryu, S. W., Lee, J. G., & Kim, H. J. (2020). Design, Fabrication, and Analysis of Flapping and Folding Wing Mechanism for a Robotic Bird. Journal of Bionic Engineering, 17(2), 229–240.

Sen, Y., & Zhongsheng, W. (2017). Quad-Rotor UAV Control Method Based on PID Control Law. 2017 International Conference on Computer Network, Electronic and Automation (ICCNEA), 418–421.

Tuna, T., Ertug Ovur, S., Gokbel, E., & Kumbasar, T. (2020). Design and development of FOLLY: A self-foldable and self-deployable quadcopter. Aerospace Science and Technology, 100, 105807.

Vargas, G. O., Hintz, C., Carrillo, L. R. G., Munoz Palacios, F., & Espinoza Quesada, E. S. (2015). Dynamic modeling of a multi-rotorcraft UAS with morphing capabilities. 2015 International Conference on Unmanned Aircraft Systems (ICUAS), 963–971.

Zhao, N., Luo, Y., Deng, H., & Shen, Y. (2017). The deformable quad-rotor: Design, kinematics and dynamics characterization, and flight performance validation. 2017 IEEE/RSJ International Conference on Intelligent Robots and Systems (IROS), 2391–2396.

Yue Zan is currently pursuing her Master's degree at the school of Mechanical Engineering, Southwest Jiaotong University, Chengdu, China. She received her B.S. degree from Hengshui College, Hengshui, China, in 2020. Her main research interests are in the areas of artificial intelligence and robotics research, variable structure drones, and environmental perception.

Xingguo Song, Ph.D., graduated from Harbin Institute of Technology, School of Mechanical and Electrical Engineering, majoring in Mechanical Design and Theory, is a visiting scholar at Rice University and a postdoctoral fellow at Johns Hopkins University, USA. His main research interests are intelligent robotics, UAV path planning, bionic robotics, and computer vision.

Lulu Gong studies at the School of Mechanical Engineering at Southwest Jiaotong University, and her research direction is autonomous drone landing technology.

Qiu Hou is currently studying in the School of Mechanical Engineering at Southwest Jiaotong University, and his main research interests are autonomous exploration and map building of UAVs in unknown environments.

Jie Tang is currently a graduate student in the School of Mechanical Engineering at Southwest Jiaotong University and his research interests are in UAV control and UAV path planning.